

RECEIVED  
JAN 10 2000  
OSTI

## Measurement and Calculation of Recoil Pressure Produced During CO<sub>2</sub> Laser Interaction with Ice

V. V. Semak\*, G. A. Knorovsky\*\*, D. O. MacCallum\*\*, D. R. Noble\*\*,  
and M. Kanouff@

\*Pennsylvania State University, ARL, State College, PA 16804  
Sandia National Laboratories,

\*\*Albuquerque, NM 87185 & @Livermore, CA 94551

### Abstract

Evaporation is a classical physics problem, which, because of its significant importance for many engineering applications, has drawn considerable attention by previous researchers. Classical theoretical models [Ya. I. Frenkel, *Kinetic Theory of Liquids*, Clarendon Press, Oxford, 1946] represent evaporation in a simplistic way as the escape of atoms with highest velocities from a potential well with the depth determined by the atomic binding energy. The processes taking place in the gas phase above the rapidly evaporating surface have also been studied in great detail [S. I. Anisimov and V. A. Khokhlov, *Instabilities in Laser-Matter Interaction*, CRC Press, Boca Raton, 1995]. The description of evaporation utilizing these models is known to adequately characterize drilling with high beam intensity, e.g.  $>10^7$  W/cm<sup>2</sup>. However, the interaction regimes when beam intensity is relatively low, such as during welding or cutting, lack both theoretical and experimental consideration of the evaporation. It was shown recently that if the evaporation is treated in accordance with Anisimov et.al.'s approach, then predicted evaporation recoil should be a substantial factor influencing melt flow and related heat transfer during laser beam welding and cutting. To verify the applicability of this model for low beam intensity interaction, we compared the results of measurements and calculations of recoil pressure generated during laser beam irradiation of a target. The target material used was water ice @  $-10^\circ\text{C}$ . The displacement of a target supported in a nearly frictionless air bearing under irradiation by a defocused laser beam from a 14 kW CO<sub>2</sub> laser was recorded and Newton's laws of motion used to derive the recoil pressure.

### 1. Introduction and Background

While efforts to simulate laser welding and cutting were started almost 30 years ago, only in recent years has great progress been made. However, a detailed analysis of the state of laser welding/cutting simulations is beyond the scope of this article. Here we only point out that the reason for the lack of progress was due to an inadequate physical picture of the laser welding/cutting process. This inadequate physical model was based upon a number of erroneous assumptions including: 1) belief that the pressure inside the keyhole was equal to the surface tension pressure, leading to the further assumptions that 2) the keyhole is in steady state, and 3) the melt flow around the keyhole has a velocity comparable to the beam translation speed [1,2]. Also, 4) the evaporation recoil pressure was either ignored or 5) assumed to be insignificant compared to the surface tension

## **DISCLAIMER**

**This report was prepared as an account of work sponsored by an agency of the United States Government. Neither the United States Government nor any agency thereof, nor any of their employees, make any warranty, express or implied, or assumes any legal liability or responsibility for the accuracy, completeness, or usefulness of any information, apparatus, product, or process disclosed, or represents that its use would not infringe privately owned rights. Reference herein to any specific commercial product, process, or service by trade name, trademark, manufacturer, or otherwise does not necessarily constitute or imply its endorsement, recommendation, or favoring by the United States Government or any agency thereof. The views and opinions of authors expressed herein do not necessarily state or reflect those of the United States Government or any agency thereof.**

## **DISCLAIMER**

**Portions of this document may be illegible in electronic image products. Images are produced from the best available original document.**

gradient or buoyancy mechanisms of flow generation. It was also believed that 6) the surface of the melt exposed to the laser beam was at a fixed temperature equal to the irradiated material's boiling temperature [3]. Finally, 7) it was believed that the propagation of the keyhole in laser welding and the cutting front in laser cutting was solely due to evaporation of material [4]. We will not attempt to provide a complete list of references on these subjects for lack of space

Since ~1970 it has been known from laser drilling research that the intense evaporation of a metal surface exposed to a laser beam induces substantial recoil pressure on the melt surface. The recoil pressure causes melt expulsion from the interaction zone and creation of a crater [5]. A natural extension of this evaporation-induced recoil pressure crater formation mechanism in laser drilling is the propagation of a cutting front or a keyhole in welding. Thus, laser welding can be represented schematically as shown in Figure 1 [6]. A similar picture, without a weld pool, which would typically be blown away through the bottom of the kerf, can be drawn for laser cutting.

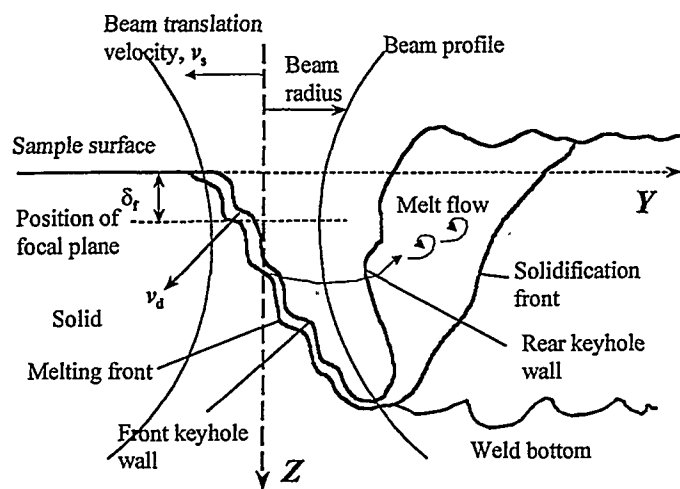


Figure 1. Schematic of laser welding.

The laser-induced recoil pressure expels melt produced at the front part of the keyhole or cutting front, and therefore the melting front propagates forward. Calculations [7,8] performed in accordance with Anisimov's theory show that for typical welding/cutting conditions the recoil pressure produces melt flow with velocities as high as several meters per second. Such melt flow obviously has a substantial effect on the thermal field [8,9]. Attempts were made to account for this effect in previous models assuming conduction heat transfer by anisotropic or artificially increased conductivity values. A significant algorithmic change is that prediction of penetration depth in welding and cutting will now require the calculation of the shape of the front part of the keyhole (or cutting front) rather than choosing an appropriate heat source power distribution to represent the keyhole. The power distribution of the heat source was defined in an ad hoc manner by the various authors, usually having a shape approximating the final weld fusion zone or keyhole (often an inverted conical shape).

Based upon the above discussion, there should be particular interest in determining the recoil pressure, since it is a dominating factor in inducing melt flow in

concentrated energy beam welding and cutting. The theory of evaporation from condensed phase surfaces has been one of the classical problems of physics. The recent increase of interest in this problem is related to development and wide use in industry of high energy flux heat sources such as lasers and electron beams. Indeed, evaporation from surfaces irradiated with concentrated energy beams is an important process because it influences energy input and determines melt hydrodynamics, chemical composition of the near-surface plume, gas dynamics of the vapor flux from the surface, etc. Because of industrial interest in surface modification techniques to improve corrosion, wear, fatigue and cosmetic properties, evaporation from surfaces exposed to electric arcs, flames and other heat sources is also being studied.

Usually such evaporation is described in terms of greatly simplified theoretical models [10-13]. These models treat evaporation as a single particle model in which the fastest atoms escape from a potential well of depth equal to the constant binding energy  $U_0$ . Such a description of evaporation is an obvious oversimplification. In reality, the binding energy is not a fixed quantity, because it depends on the structure of the immediate environment of the atom in question. Recent theoretical work [14,15] showed that fluctuations of binding energy in the surface layers play an important role in evaporation. If the fluctuations are accounted for, a significant additional contribution to the evaporating flux comes from atoms whose energy is of the same magnitude as the mean thermal energy. Since under typical conditions for arc, laser or e-beam welding, or laser and flame cutting,  $k \ll U_0$ , the evaporation flux predicted by the new theory changes substantially compared to that predicted by traditional theory [10-13].

Developments in the molecular-dynamics simulation approach [15] promise more realistic simulations of evaporation from surfaces exposed to high heat fluxes. The results of such simulations will provide crucial input parameters for the calculation of vapor flow properties using Anisimov's detailed model of the gas phase processes [16,17]. This model provides such important vapor flow parameters as density, velocity and temperature. It also considers condensation and droplet formation in supersaturated vapor flow. Finally, and of interest here, this model allows calculation of the evaporation recoil pressure acting on the surface of the melt.

Because the recoil pressure is the main mechanism which induces melt flow and as such determines the welding/cutting penetration, temperature distribution, pool instabilities, etc., the correct computation of the value of recoil pressure is very important for the simulation of laser welding and cutting. Anisimov's theory has never been verified by direct experimental measurements. Therefore the objective of our work is to attempt such verification.

## 2. Experiment

A Convergent Energy 14 kW CO<sub>2</sub> laser was used in experimental measurements of recoil pressure. The laser beam was defocussed at the surface of a frozen water sample into spotsizes of 3 mm or 6.4 mm diameter. The ice cube sample was placed at the end of a carrier floating in an air bearing (Fig.2). The evaporation induced in the sample during laser irradiation produced a recoil force, which moved the carrier and attached target. This motion was detected with a fiber-optic based displacement sensor and the signal representing the position of the cylinder in time was recorded by a digital

oscilloscope. The analysis of this signal gave displacement, allowing calculation of the velocity and acceleration. With knowledge of the carrier plus target mass this allowed calculation of the recoil force via Newton's laws of motion. Typical derived data records are shown in Fig.3. The sensor was used far beyond its linear range, but since the motion of the carrier was expected to be monotonic in direction, an extended displacement vs time record was deduced by piecewise fitting the non-linear voltage vs displacement curve using MatLab. This allowed a measurement range of about 2-3 mm with a high bandwidth (~50kHz) device. Because of this limited measurement range, the rapid acceleration of the carrier, and a slow shutter opening time (~130 ms), an intensity vs time profile had to be assumed when calculating the expected motion in a later section.

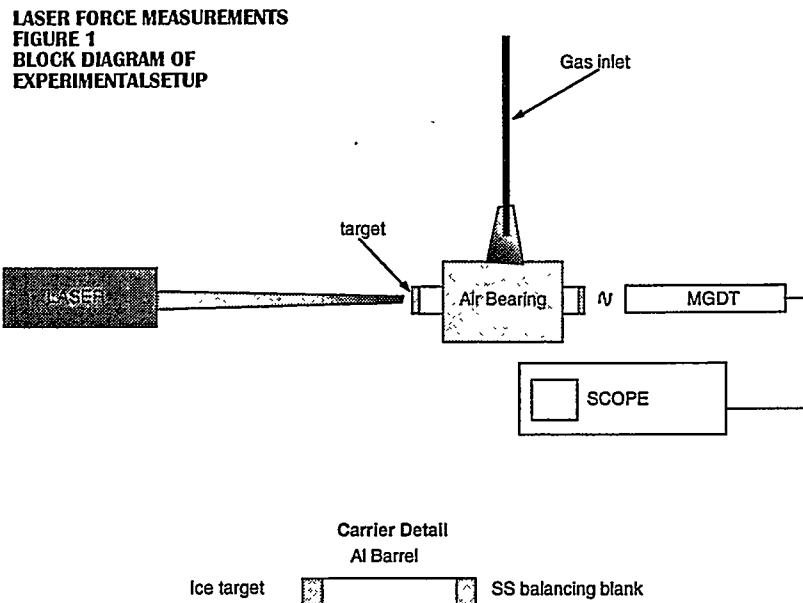


Figure 2. Schematic diagram of experimental arrangement.

These plots in Figure 3 display the smoothed fit velocity and acceleration curves with a common origin. Velocity data is a smoothed derivative of smoothed location data; Acceleration data is a smoothed derivative of the smoothed velocity data. Originally we used polynomial fits to the data, and showed that we could reasonably well recover the original voltage vs time data from the resulting acceleration vs time fit. However, since the polynomial fit routine tends to reflect the global curve, it wipes out local variations. A smoothed fit is more local, and in particular does a better job at the beginning of motion. The smoothing routine used (in Kaleidagraph) applies a Stineman function to the data. The output of this function then has a geometric weight applied to the current point and +/- 10% of the data range to arrive at the smoothed curve. Both types of derived results are given in Table 1.

A large spot diameter was chosen to ensure that at the initial stage of the interaction the vapor expansion is one-dimensional and that liquid is not expelled from the interaction zone. Unfortunately the resources available at the time did not allow monitoring the liquid motion.

Notice in Figure 3b that it takes about 20-40ms for peak acceleration to occur, inversely related to laser intensity, after which the acceleration decreases. We estimate it takes ~65 ms for the peak laser irradiance to hit the sample (time to 50% shutter opening, assuming a Gaussian beam), and twice as long to achieve full power, so complete

Table 1: Experimental conditions and derived results:

Test ID	1	2	3	4	5	6	7
<b>Laser beam parameters:</b>							
Power (kW):	4	4	4	4	4	2	6.4
Standoff distance (mm):	152	152	152	190	190	190	152
Spot diameter (mm):	3	3	3	6.4	6.4	6.4	3
Spot area (mm <sup>2</sup> ):	7.069	7.069	7.069	32.17	32.17	32.17	7.069
Power density (W/mm <sup>2</sup> ):	565.9	565.9	565.9	124.3	124.3	62.17	905.4
ice initial mass (g):	4.03	6.43	5.42	7.34	9.26	10	10.73
ice final mass (g):	2.76						
Carrier mass (g):	3.18	3.18	3.18	3.18	3.45	3.45	3.45
Shield mass (g):	0	2.17	2.17	3.16	3.16	3.16	3.16
Total initial mass (g):	7.21	11.78	10.77	13.68	15.87	16.61	17.34
<b>Polynomial fit data:</b>							
Beginning of motion (s):	0.073	0.066	0.074	0.07	0.077	0.053	0.078
max velocity (mm/s):	112.1	51.5	55.47	61.49	54.38	39.7	62.87
Time at max vel (s):	0.099	0.113	0.11	0.109	0.112	0.116	0.107
Time at max vel - beginning of motion (s):	0.026	0.047	0.036	0.039	0.035	0.063	0.03
max acceleration (mm/s <sup>2</sup> ):	5251	1994	2339	2510	2157	919	2549
Time at max accel (s):	0.086	0.099	0.096	0.096	0.099	0.067	0.093
Time at max accel - begin motion (s):	0.013	0.034	0.022	0.026	0.022	0.014	0.015
<b>"smoothed" fit data:</b>							
Beginning of motion (s):	0.074	0.065	0.074	0.054	0.073	0.052	0.075
max velocity (mm/s):	99.7	50.6	50.75	63.3	59.4	39.1	58.2
Time at max velocity (s):	0.1	0.116	0.113	0.111	0.116	0.125	0.111
max acceleration (mm/s <sup>2</sup> ):	4600	1412	1580	1786	1668	969	2120
Time at max acceleration (s):	0.082	0.102	0.096	0.094	0.108	0.092	0.087
<b>"polynomial" results:</b>							
Peak force max: (=init mass x peak accel) in kg m/s <sup>2</sup> (N):	0.038	0.023	0.025	0.034	0.034	0.015	0.044
Peak force min: (=carrier + brass mass x peak accel) in kg m/s <sup>2</sup> (N):	0.031	0.011	0.013	0.016	0.014	0.006	0.017
Peak pressure (=peak force/spot area in N/m <sup>2</sup> = Pa):	5356	3323	3563	1067	1064	474.5	6254
<b>"smoothed" results:</b>							
Peak force max: (=init mass x peak accel) in kg m/s <sup>2</sup> (N):	0.033	0.017	0.017	0.024	0.026	0.016	0.037
Peak force min: (=carrier + brass mass x peak accel) in kg m/s <sup>2</sup> (N):	0.027	0.008	0.008	0.011	0.011	0.006	0.014
Peak pressure (=peak force/spot area in N/m <sup>2</sup> = Pa):	4692	2353	2407	759.5	822.9	500.3	5201
N.B.: 100kPa ~ 1 atm							
<b>"polynomial" results:</b>							
Peak pressure/power density (Pa-mm <sup>2</sup> /W):	9.465	5.873	6.297	8.584	8.559	7.632	6.907
<b>"smoothed" results:</b>							
Peak pressure/power density (Pa-mm <sup>2</sup> /W):	8.292	4.158	4.254	6.108	6.618	8.048	5.744

absorption of the beam cannot be occurring, perhaps because of the water vapor plume being generated.

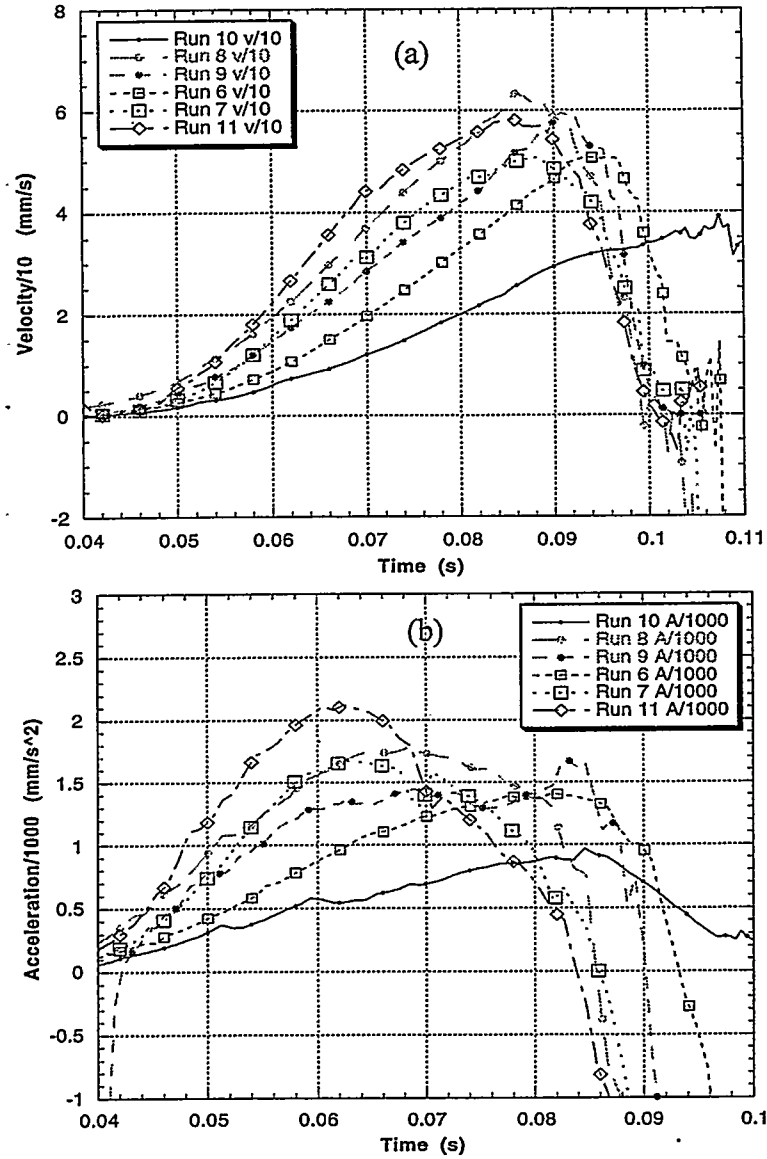


Figure 3. Calculated a) velocity (x 0.1) and b) acceleration(x 0.001) vs. time in seconds.

### 3. Numerical simulation of evaporation recoil

The dependencies of position vs. time were numerically calculated and compared to the measurements. The calculation scheme included one-dimensional calculation of the water surface temperature:

$$\frac{\partial T}{\partial t} + V_{dv} \frac{\partial T}{\partial z} = \frac{k_1}{\rho_1 c_1} \left( \frac{\partial^2 T}{\partial z^2} \right). \quad (1)$$

Here subscript “l” refers to the liquid phases and  $\rho$ ,  $c$ ,  $T$ , and  $k$  are the density, specific heat, temperature and heat conductivity, respectively, while  $V_d$  is the velocity of the evaporation front propagating into the sample. The coordinate system is such that the x-y plane coincides with the sample surface and the z-axis is normal to the surface and parallel to the laser beam.

A mixed-type boundary condition was applied on the liquid - vapor boundary

$$-k \left. \frac{\partial T}{\partial z} \right|_{\text{surf}} + \rho V_{dv} L_v = (1 - R) I_{\text{laser}}, \quad (2)$$

where  $k$  is the heat conductivity of solid or liquid phase,  $\left. \frac{\partial T}{\partial z} \right|_{\text{surf}}$  is the temperature gradient at the surface,  $R(\phi)$  is the angular dependent reflection coefficient for the laser wavelength, and  $I_{\text{laser}}$  is the intensity of the laser beam at the surface. For typical welding conditions the melt surface temperature is much lower than the critical temperature and the energy of evaporation of a single atom,  $U$ , can be approximated as a constant. Then the evaporation velocity,  $V_{dv}$ , can be expressed by the equation (1)

$$V_{dv} = V_0 \exp\left(-\frac{U}{kT_{\text{surf}}}\right), \quad (3)$$

where  $V_0$  is a coefficient of magnitude of the sound velocity, and  $T_{\text{surf}}$  is the local surface temperature. Note that this boundary condition (2,3) differs from the commonly used “Problem of Stefan” boundary condition. The surface temperature is not fixed at the boiling point; it depends on the absorbed intensity.

The solution of equation (1) with boundary conditions (2,3) determines the temperature of the water surface. Then the recoil pressure can be computed using the equation:

$$p_r = AB_0 T_{\text{surf}}^{-1/2} \exp\left(-\frac{U}{kT_{\text{surf}}}\right), \quad (4)$$

where  $A$  is a coefficient dependent on ambient pressure, and  $B_0$  is a known empirical constant with value  $1.44e+13$  in cgs units.

After the recoil pressure is calculated, the sample acceleration (lower bound) can be determined assuming that at the initial stage of the interaction evaporation does not reduce sample mass (given the other experimental difficulties it didn't seem worthwhile to worry about mass loss during the measurement window):

$$a = \int_0^t p_r(T_{\text{surf}}(t)) s dt, \quad (5)$$

where  $s$  is the area of the laser spot at the ice surface (which varies because of the shutter and part standoff variation). Further integration over time provides sample velocity and position histories. Typical results of calculations (carried out by programming the above equations into MatLab) are presented in Fig. 4 @ 4kW and 6.4 mm beam diameter.

#### 4. Analysis of Results

Comparison of the measured values of velocity, acceleration and pressure with those calculated from Anisimov's theory show very poor agreement. The calculated values are in all cases far larger (by at least an order of magnitude).

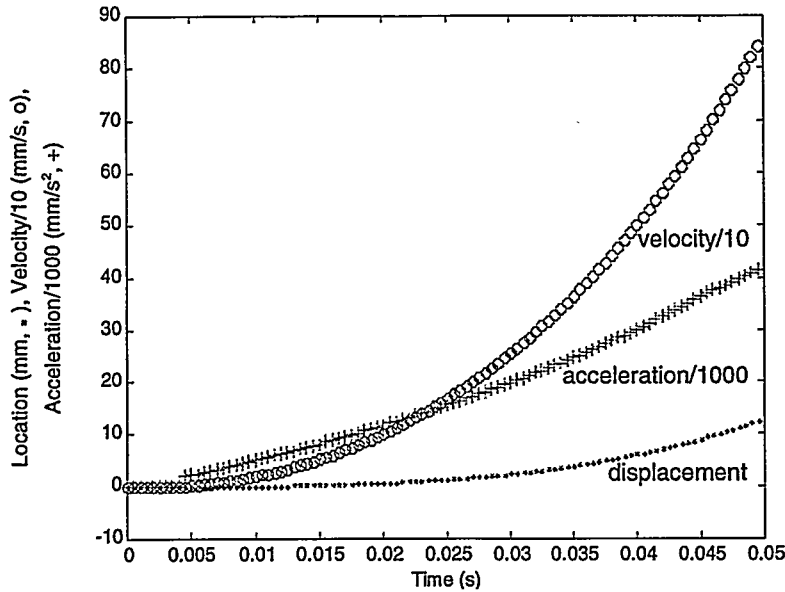


Figure 4. Calculated results comparable (same x and y scales) to measured values in Figure 3

Because the samples were either drilled through or completely fragmented during the experiments (with very impressive plumes being generated!), it was clear that significant energy transfer occurred. Possible reasons for the disagreement include uncertainty in the value of the constant A, and the likelihood of a reduced beam intensity at the surface of the ice because of plume absorption and defocusing ('blooming') effects. It is also very possible that the extensive melting and fragmentation of the samples may have allowed absorbed energy to be dissipated in other than momentum transfer parallel to the beam direction, violating the one dimensional force and heat flow assumption. Consistent with this hypothesis, trial #1, which was the only run which didn't fragment the ice (it only drilled a through-hole), gave the largest measured values for velocity and acceleration and second highest for pressure. It is clear that further experimentation will be needed, with: a) a faster shutter, b) samples with a reinforcing ring to prevent fragmentation and c) high speed video observation of the ice's flow behavior. Unfortunately, one cannot state unequivocally at this point that Anisimov's model has been either verified or disproved.

## 5. Conclusions

Experiments have been conducted upon ice with the intent of measuring the recoil pressures generated by laser irradiation. Values determined were in the range of a few hundredths of an atmosphere. A comparison was made with Anisimov's model of the pressure generated under laser irradiation. Poor agreement was found; however, experimental difficulties may have prevented a fair test. Further work is planned which will remedy two major experimental faults identified, i.e. fragmentation of the samples and a slow shutter, and provide concurrent high speed video observations.

## 6. Acknowledgement

This work was supported by the U.S. Department of Energy under contract DE-AC04-94AL85000. Sandia is a multiprogram laboratory operated by Sandia Corporation, a Lockheed Martin Company, for the U.S. Department of Energy. The authors would also like to thank Russell Knee and Edward Good of ARL for help in the laser experimentation.

## 7. References

1. A. Kaplan, "A Model of Deep Penetration Laser Welding Based on Calculation of the Keyhole Profile", *J. of Phys. D: Applied Physics*, vol. 27, (1994), pp.1805 - 1814.
2. P.G. Klemens, "Heat Balance and Flow Conditions for Electron Beam and Laser Welding", *J. App. Phys.*, vol. 47, no. 5, pp. 2165-2174, May 1976; J. Frenkel, *Kinetic Theory of Liquids*, Dover Publications, Inc. New York, 1955.
3. A. Kar and J. Mazumder, "Mathematical Modeling Of Key-Hole Laser Welding", (1995), *J. Applied Physics*, vol. 78, (11), pp.6353-6360.
4. J. Xie and A. Kar, "Mathematical Modeling Of Melting During Laser Materials Processing", (1997), *J. Appl. Phys.*, vol. 81, (7), pp.3015 - 3022.
5. M. von Almen (1976) *J. Appl. Phys.* vol. 47, p. 5460.
6. V. V. Semak, W. D. Bragg, B. Damkroger, and S. Kempka, "Transient Model for the Keyhole During Laser Welding", (1999), *J. Phys. D:Appl.Phys.* vol. 32, pp.L61-L64
7. A. Matsunawa and V. Semak, "Simulation of the Front Keyhole Wall Dynamics During Laser Welding", *J. of Physics D: Applied Physics*, (1997), vol. 30, p.798.
8. V. Semak and A. Matsunawa, "Role of the Recoil Pressure in Energy Balance During Laser Welding", *Journal of Physics D: Applied Physics*, (1997), vol 30, p.2541.
9. V. Semak, B. Damkroger, and S. Kempka, "Temporal Evolution Of The Temperature Field In The Beam Interaction Zone During Laser Material Processing", *J.Phys.D:Appl. Phys.*, (1999), vol. 32, pp.1819-1825.
10. J. Frenkel, *Kinetic Theory of Liquids*, Dover Publications, Inc. New York, 1955.
11. O. Knake and I. N. Stranskii, *Sov. Phys. Usp.* Vol 2, (1959).
12. J. P. Hirth and G. M. Pound, *Condensation and Evaporation: Nucleation and Growth Kinetics*, Pergamon Press, Oxford, 1963.
13. S. I. Anisimov and V. V. Zhakhovskii, "Evaporation of a Liquid", *JETP Lett.*, vol. 57, no. 2, 25 January 1993, pp. 99 -102.
14. V. V. Zhakhovskii and S. I. Anisimov, "Molecular-Dynamics Simulation of Evaporation of a Liquid", *JETP*, vol. 84(4), April 1997, pp. 734-745.
15. S. I. Anisimov, "Vaporization Of Metal Absorbing Laser Radiation", 1968, *Sov. Phys. - JETP*, vol. 27, p. 182.
16. S.I. Anisimov and V.A. Khokhlov, *Instabilities in Laser-Matter Interaction*, CRC Press, Boca Raton, FL, 1995.